Precipitation and age hardening

MAURO PALUMBO

mauro.palumbo@unito.it
Dipartimento di Chimica
Università di Torino
Via Pietro Giuria 9 –10125 Torino

Precipitation

A phase transformation through which a second phase forms from a supersaturated solid solution as a distinct new phase, differing in composition and often in crystal structure from the host matrix.

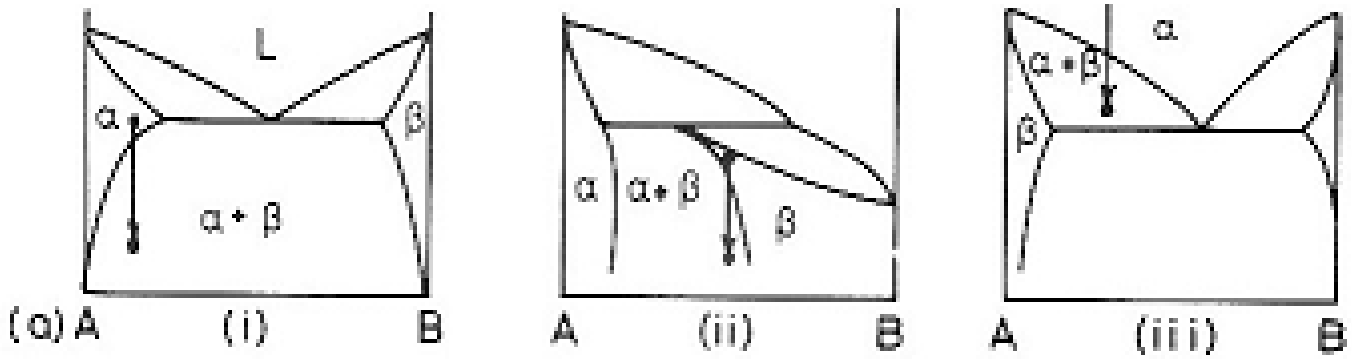

- An important example: precipitation of ferrite from austenite
- Age hardening

Precipitation of ferrite from austenite

Equilibrium phase transformation.
Nucleation is heterogeneous on gb's and inclusions.

Ferrite formation at various T's then quenching reported from (a) to (d) :

a) 'blockey' crystals or allotriomorphs, both curved and planar interfaces;

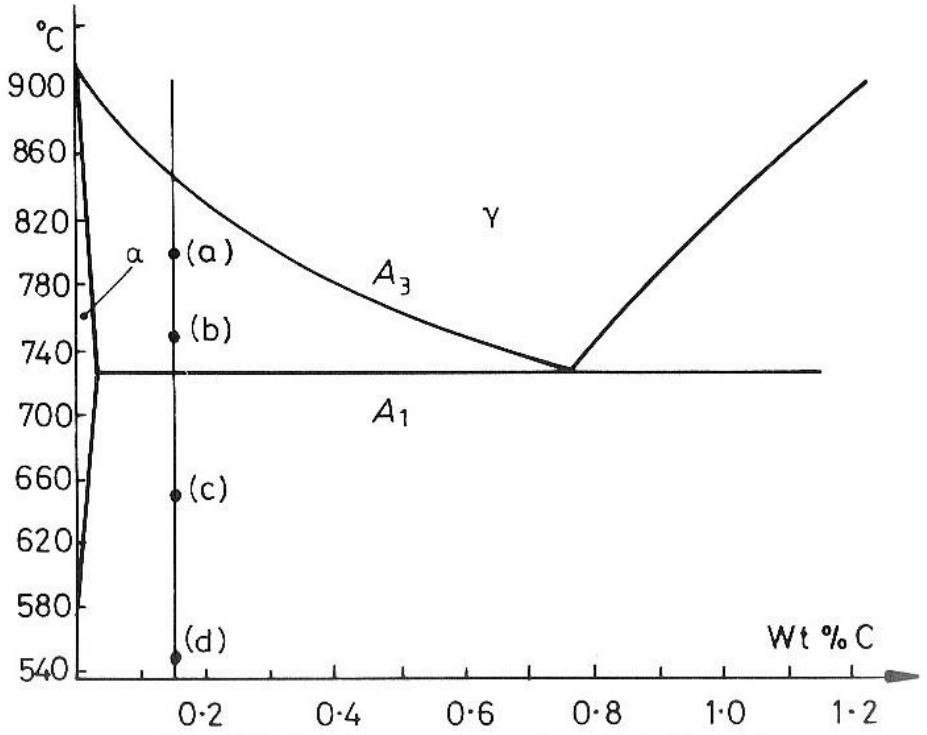

An allotriomorph has a shape which does not reflect its internal crystalline symmetry. This is because it tends to nucleate at the austenite grain surfaces, forming layers which follow the grain boundary contours. The allotriomorph is in contact with at least two of the austenite grains and will have a random orientation with one of them, but an orientation which is more coherent with the other. It may, therefore, be crystallographically facetted on one side but with a curved boundary on the other side.

Precipitation of ferrite from austenite

a) continue…

microstructures of blockey crystals

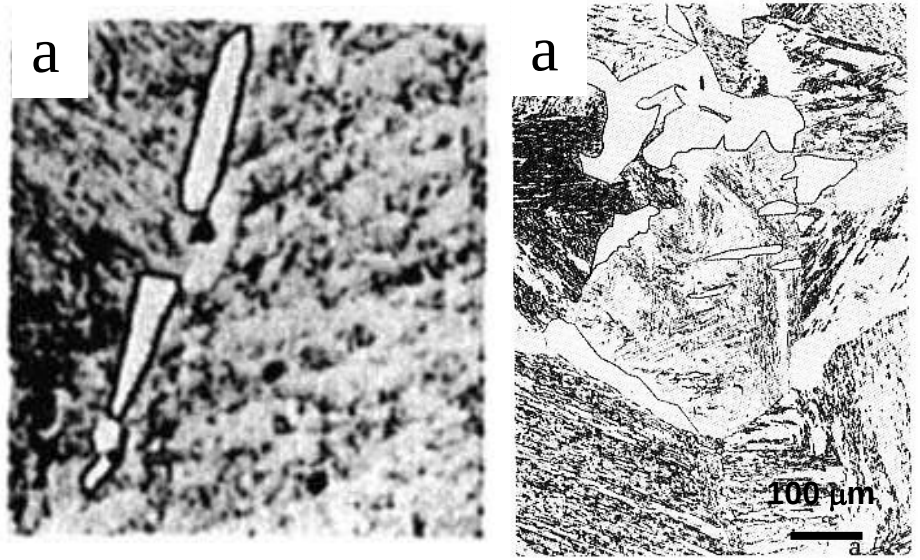

b) more blockey crystals together with plates.

Plates known as Widmanstätten morphology: lateral growth with orientation relationship. For nucleation semi-coherent interfaces lower ΔG^*. Incoherent are more mobile in growth. This is a possible reason for transition from blockey to lateral growth.

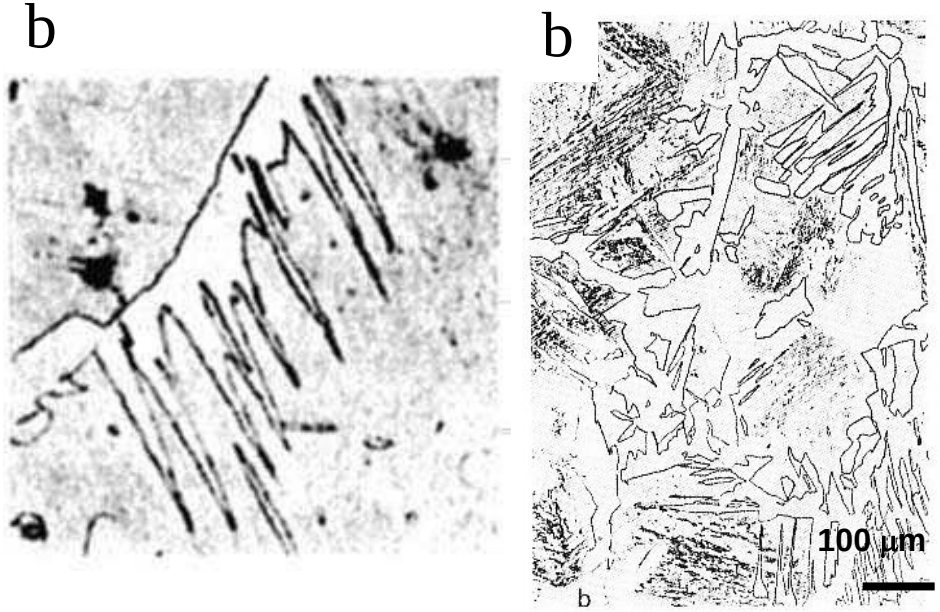

Precipitation of ferrite from austenite

b) continue…
Widmanstätten plates do not grow across the austenite grain boundaries.
Primary Widmanstätten ferrite grows directly from the austenite grain surfaces, whereas secondary Widmanstätten ferrite develops from allotriomorphs of ferrite already present in the microstructure

c) thinner plates, lateral growth;

d) ferrite barely visible. Dark areas are due to martensite.

In a) also intragranular ferrite in large grains, nucleated later.

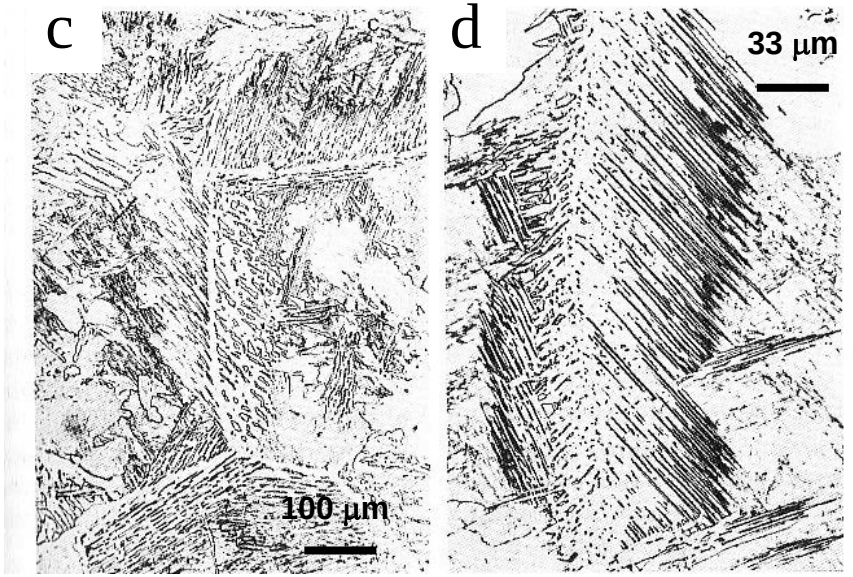

Precipitation of ferrite from austenite

Orientation relationships found in ferrous alloys:

Nishiyama-Wasserman (N-W) $(110)_{bcc}//(111)_{fcc}$, $[001]_{bcc}//[\bar{1}01]_{fcc}$

Kurdjumov-Sachs (K-S) $(110)_{bcc}//(111)_{fcc}$, $[1\bar{1}1]_{bcc}//[0\bar{1}1]_{fcc}$

(difference is ~ 5° rotation of close-packed planes)

Fit only in small areas. Irrational interfaces must be formed with ledges and misfit dislocations.

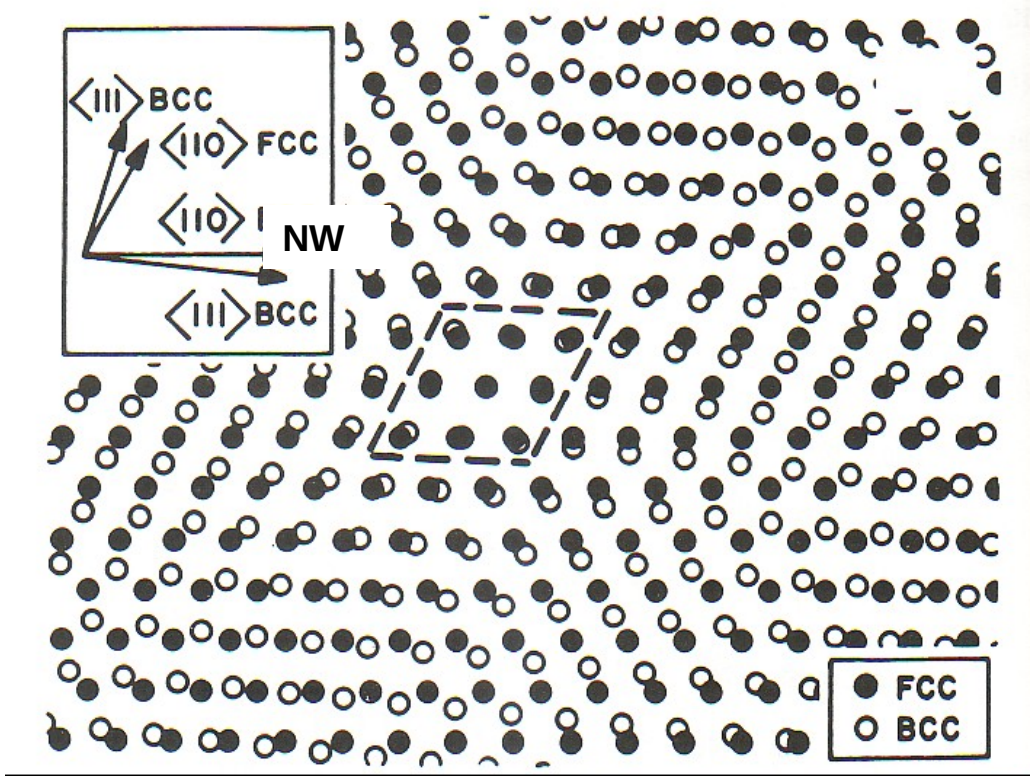

Precipitation of ferrite from austenite

In a TTT diagram for $\gamma \rightarrow \alpha$, at high T blockey gb allotriomorphs (GBA) form; below a given undercooling (T_W) ferrite takes Widmanstätten morphology.

There is an effect of grain size: with finer austenite grains, the TTT curve shifts to shorter times.

The morphologies change as a function of Carbon content as shown by zones marked on phase diagram.

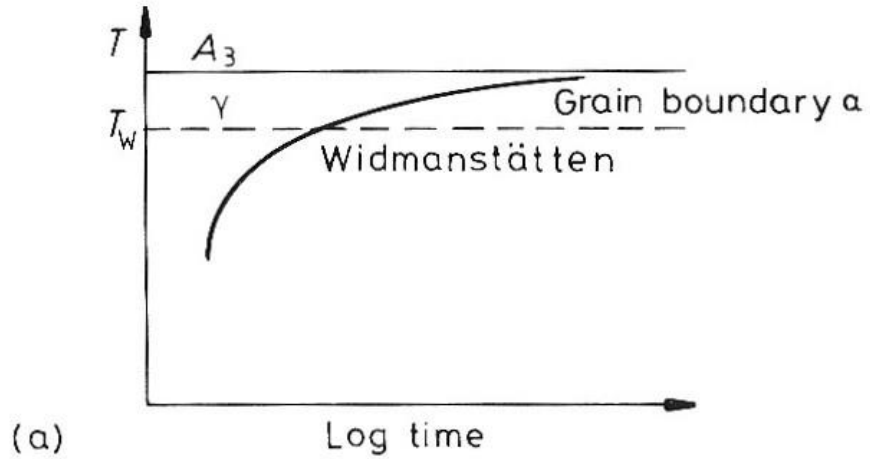

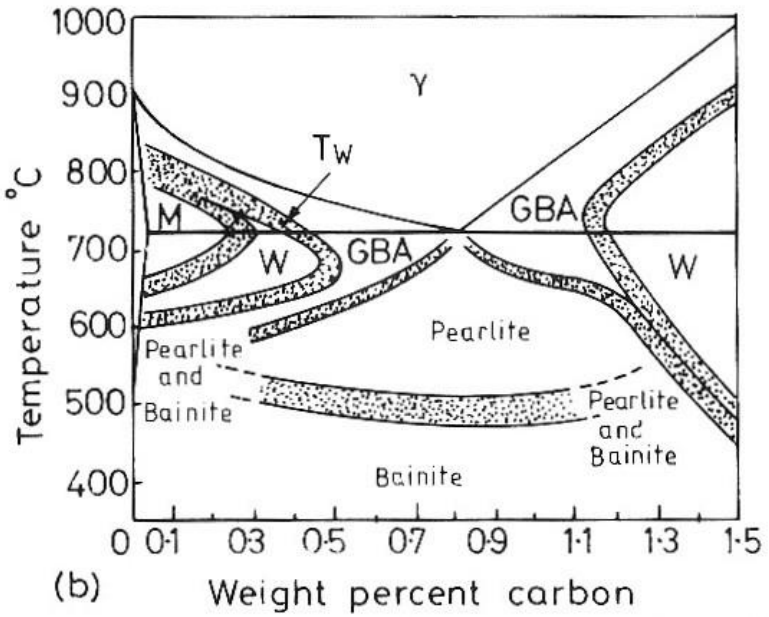

Precipitation of ferrite from austenite

Examples of microstructures in 0.23 %C, 1.2 %Mn.

Influence of γ grain size:

a) annealed at 900 ° C

b) annealed at 1150 ° C

Influence of cooling rate in 0.4%C:

c) furnace cooling

d) air cooling

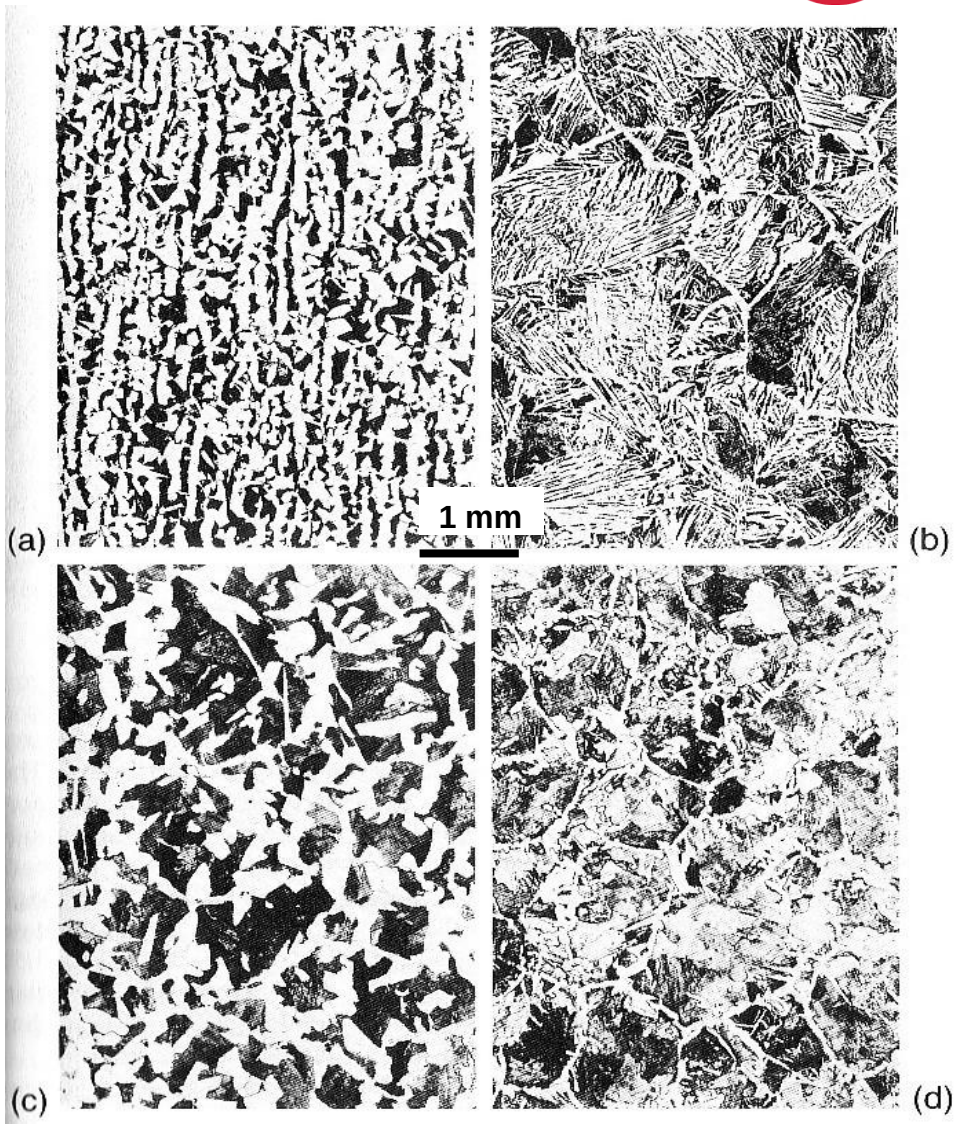

Precipitation in age hardening alloys

The **precipitates** that form during some thermal treatments **can hinder the movement of dislocations** within the crystal lattice of the metal. By impeding dislocation movement, the **precipitates increase the strength and hardness** of certain alloys, for example Al alloys. The process is called age hardening or precipitation hardening.

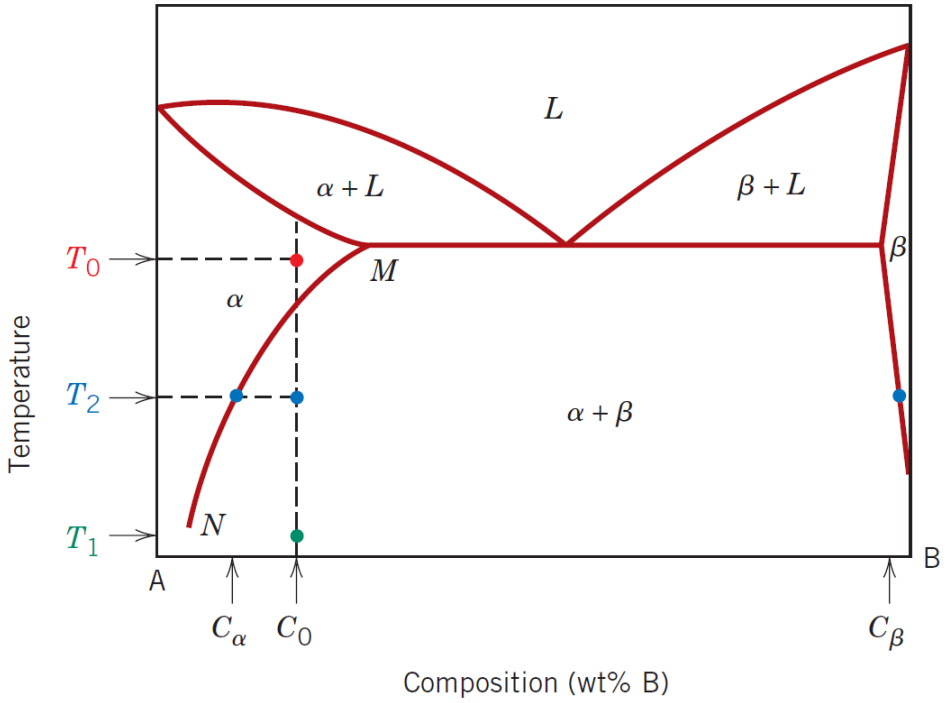

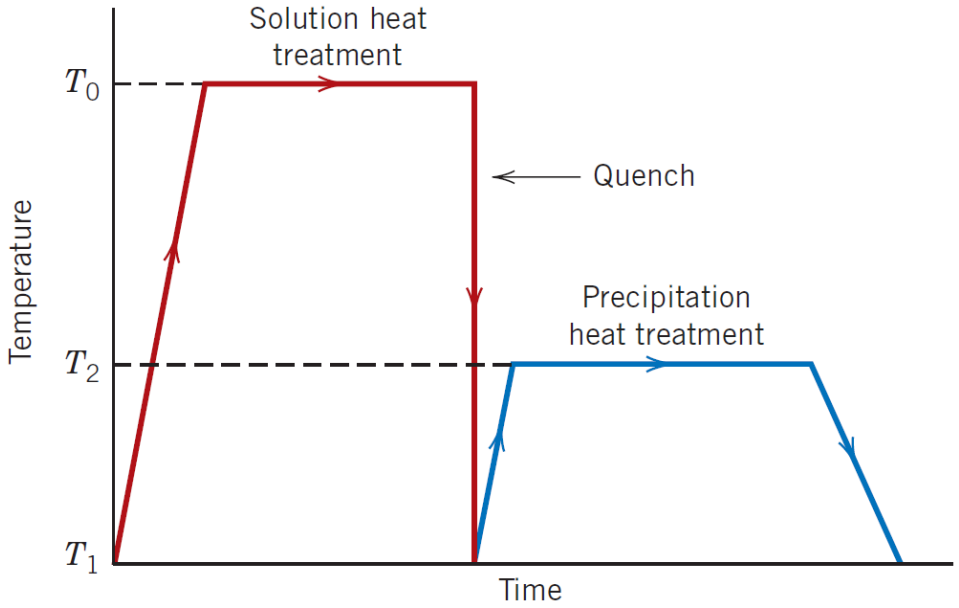

Precipitation in age hardening alloys

The sequence and the number of phases that can precipitate during age hardening can vary depending of the alloy.

Base metal	Alloy	Precipitation sequence
Aluminium	Al–Ag	GPZ (spheres) → γ′ (plates) → γ (Ag_2Al)
	Al–Cu	GPZ (discs) → θ″ (discs) → θ′ (plates) → θ ($CuAl_2$)
	Al–Cu–Mg	GPZ (rods) → S′ (laths) → S ($CuMgAl_2$) (laths)
	Al–Zn–Mg	GPZ (spheres) → η′ (plates) → η ($MgZn_2$) (plates or rods)
	Al–Mg–Si	GPZ (rods) → β′ (rods) → β(Mg_2Si) (plates)
Copper	Cu–Be	GPZ (discs) → γ′ → γ (CuBe)
	Cu–Co	GPZ (spheres) → β (Co) (plates)
Iron	Fe–C	ε-carbide (discs) → Fe_3C (plates)
	Fe–N	α″ (discs) → Fe_4N
Nickel	Ni–Cr–Ti–Al	γ′ (cubes or spheres)

Precipitation in age hardening alloys: Al-Cu

Phase diagram displays large variation of solubility of θ phase (Al_2Cu) as a function of temperature.

1) annealing at about 520 ° C for full solubilization,

2) quench to RT freezes the supersaturated solid solution,

3) annealing at low-intermediate temperature (from RT to 180 ° C) causes precipitation of intermediates,

4) sequence is

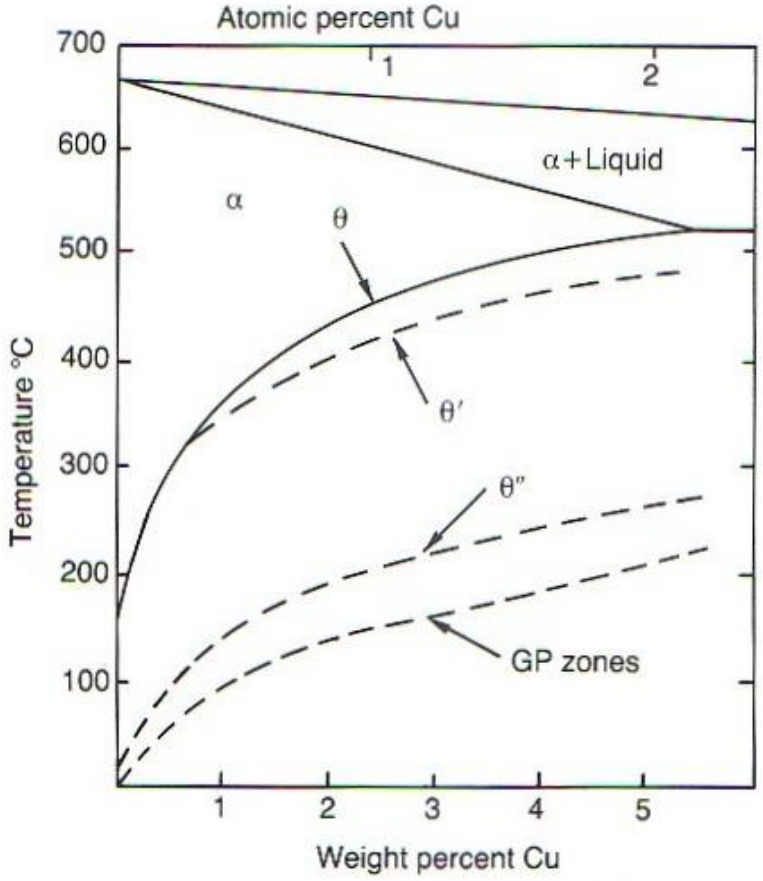

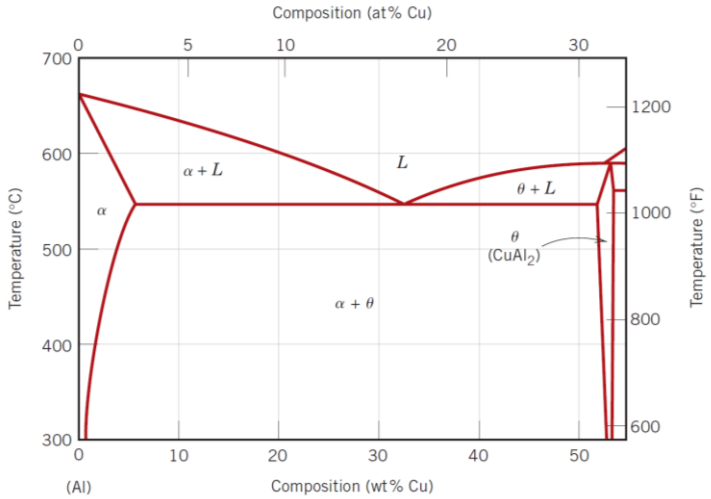

$$\alpha_0 \rightarrow \alpha_1 + \text{GP zones} \rightarrow \alpha_2 + \theta\text{“} \rightarrow \alpha_3 + \theta\text{'} \rightarrow \alpha_4 + \theta$$

Guinier-Preston zones

Coherent Cu-rich agglomerates, disc shaped (reduce strain energy) ~10 nm in diameter, ~2 lattice plane thick, aligned parallel to (200) planes, spacing between them ~10 nm.

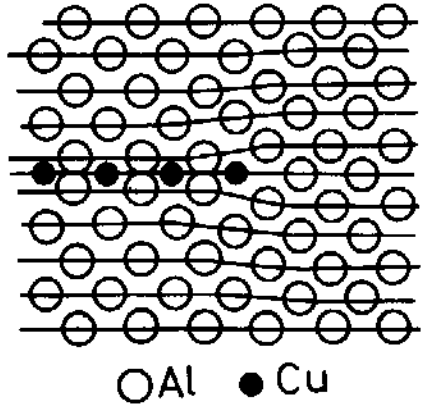

(200) plane intersected by GP-zone

Zones induce coherency misfit strain perpendicular to them. Unconstrained, δ, and constrained, ε, misfits are

$$\delta = \frac{a_\beta - a_\alpha}{a_\alpha}$$

$$\varepsilon = \frac{a'_\beta - a_\alpha}{a_\alpha} \cong \frac{2}{3}\delta$$

ΔG_S proportional to δ^2.

According to misfit in different alloys, zones will have varied shape. Also crystallographic direction matter: cubic metals are soft on <100> and strong on <111>.

Precipitation in age hardening alloys

Constrained misfit due to strain in precipitates where lattice constant becomes a'_β

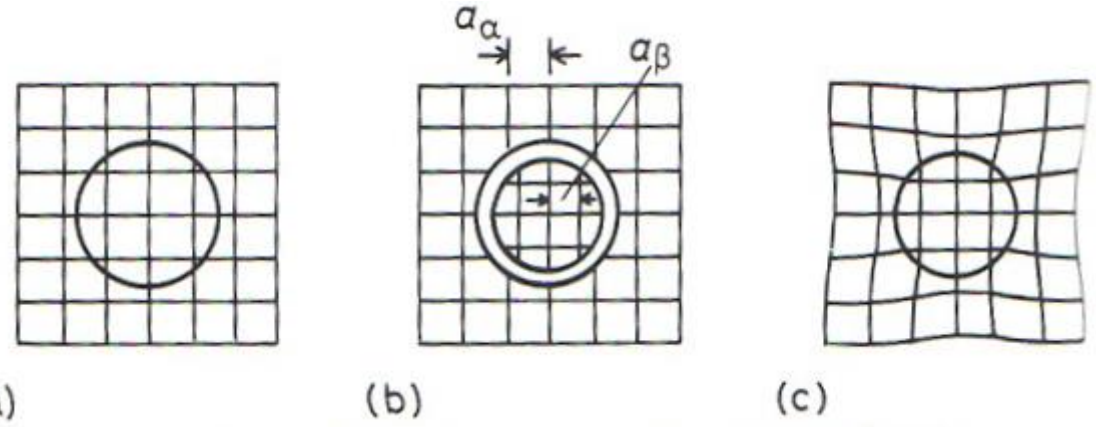

$$\delta = \frac{a_\beta - a_\alpha}{a_\alpha}$$

$$\varepsilon = \frac{a'_\beta - a_\alpha}{a_\alpha} \cong \frac{2}{3}\delta$$

Elastic strain energy for isotropic matrix + one precipitate (G, shear modulus; V, volume of unconstrained hole)

$$\Delta G_s \cong 4G\delta^2 V$$

If δ < 5%, zone spherical, otherwise disc shaped.

	Al	Ag	Zn	Cu	Mg
Atomic radius, Å	1.43	1.44	1.38	1.28	1.50
δ misfit, %		+0.7	-3.5	-10.5	-5.0
zone shape		sphere	sphere	disc	sphere

Transition and equilibrium phases

Transition phases are:

- α-matrix: fcc-supersaturated solid solution;

- θ“ tetragonal unit cell (distorted fcc, Al_3Cu); Al and Cu atoms ordered on (001) planes; fully coherent plates: orientation relationship:
$(001)_{\theta“} \parallel (001)_{\alpha}$
$<100>_{\theta“} \parallel <100>_{\alpha}$

size: ~100 nm in diameter, ~10 nm thick; some Authors describe it as thickened GP zone; coherency strain ⊥ to plate.

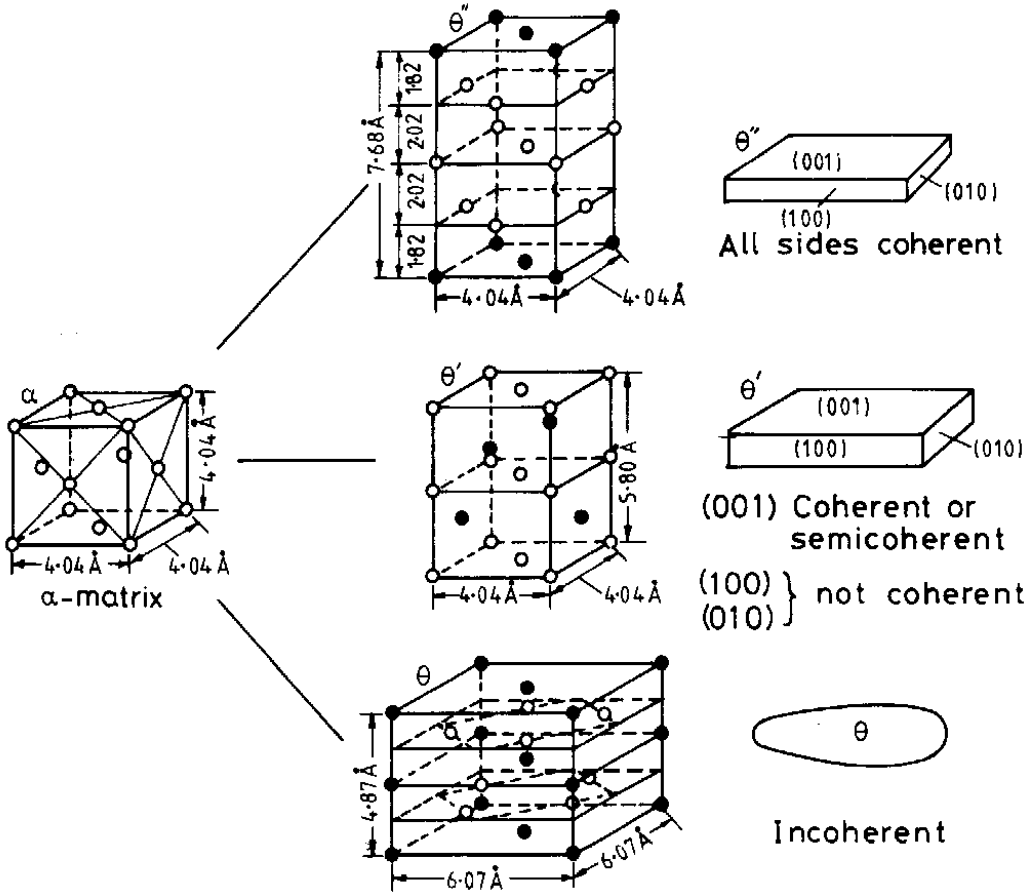

from Porter-Easterling

Transition and equilibrium phases

- θ’ tetragonal; composition $CuAl_2$; coherent on $(001)_{\theta'}$ planes; (100) and (010) plane have large misfit with matrix; plate shape.

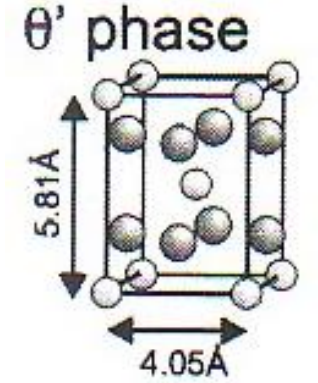

Structure refined with respect to P.-E. book

distorted CaF_2 type (tetragonal), 1.5% coherency strain.

Equilibrium phases are

- α-matrix: ~ pure Al

- θ complex tetragonal, incoherent, large crystal size.

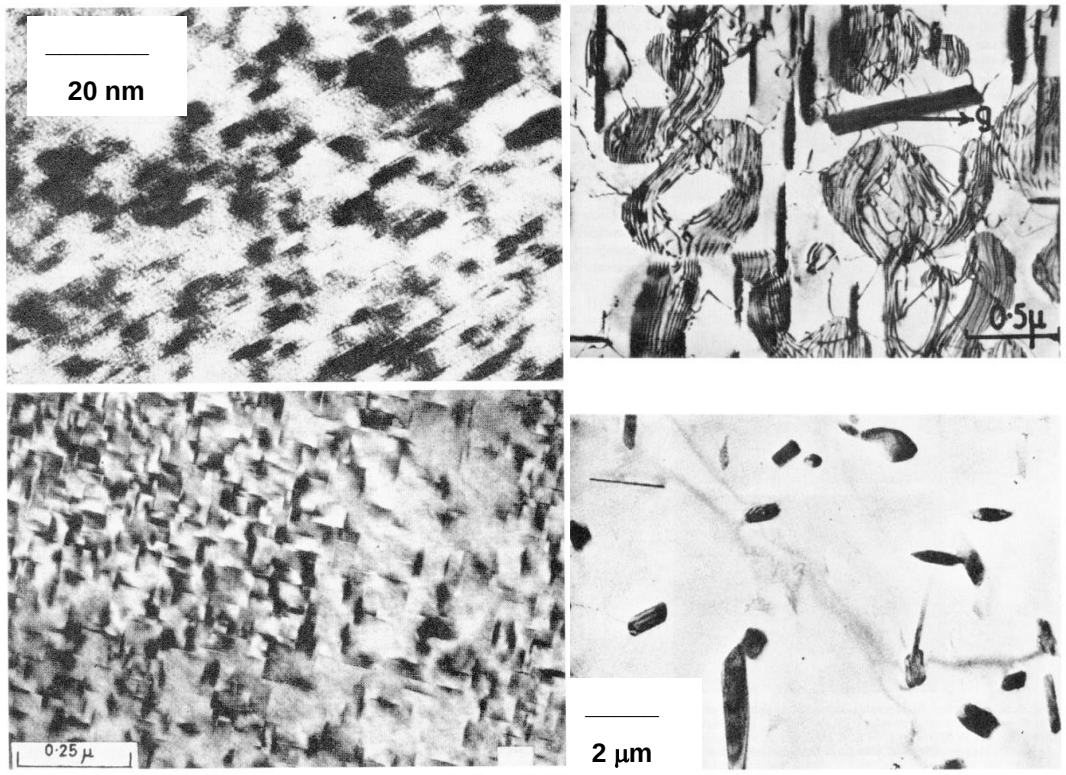

Free energies and metastable equilibria

Supersaturated fcc solid solution and GP zones on same curve because of same structure. Free energy of θ“, θ’ and θ phases as for compounds. Subscripts n between 0 and 3 indicate metastable equilibria with decreasing level of supersaturation. Subscript n = 4 indicates equilibrium state.

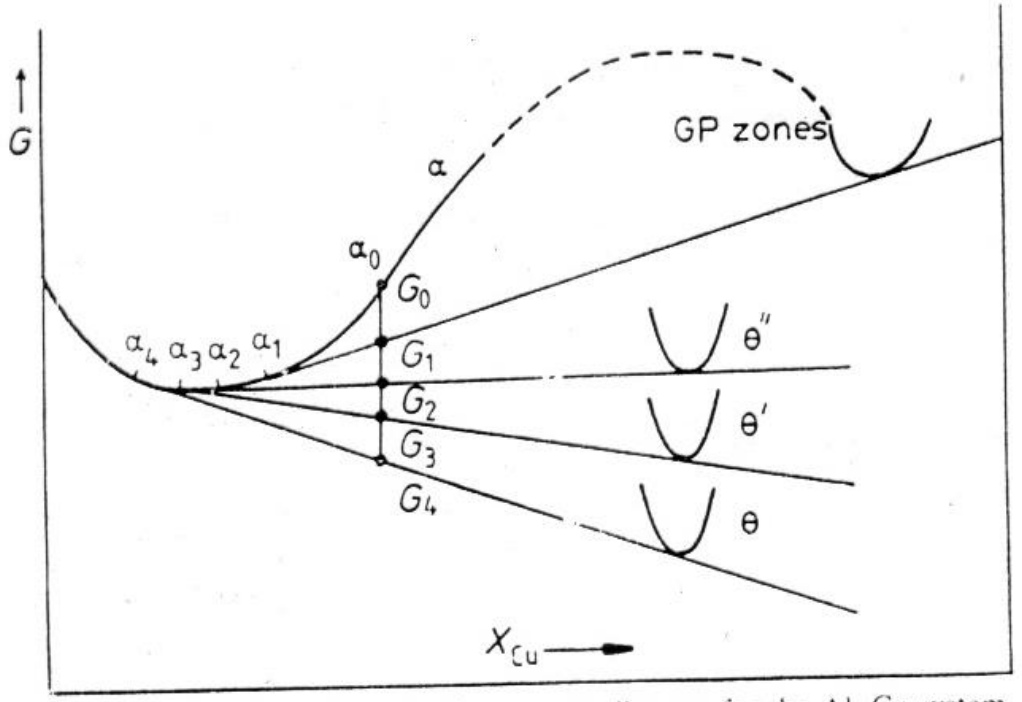

Fig. 5.27 A schematic molar free energy diagram for the Al–Cu system.

Free energy steps ($\Delta G_n = G_n - G_{n-1}$) drive each transformation. Activation barriers low because of coherence between transition phases and matrix.

Precipitation kinetics

Enhanced diffusion rate caused by excess vacancies favours formation of GP-zones which are potent nucleation sites for θ“.

θ’ nucleates on dislocations which reduce misfit strain. Growth occurs at the expense of θ“ by means of diffusion within the matrix (from α_2 to α_3)

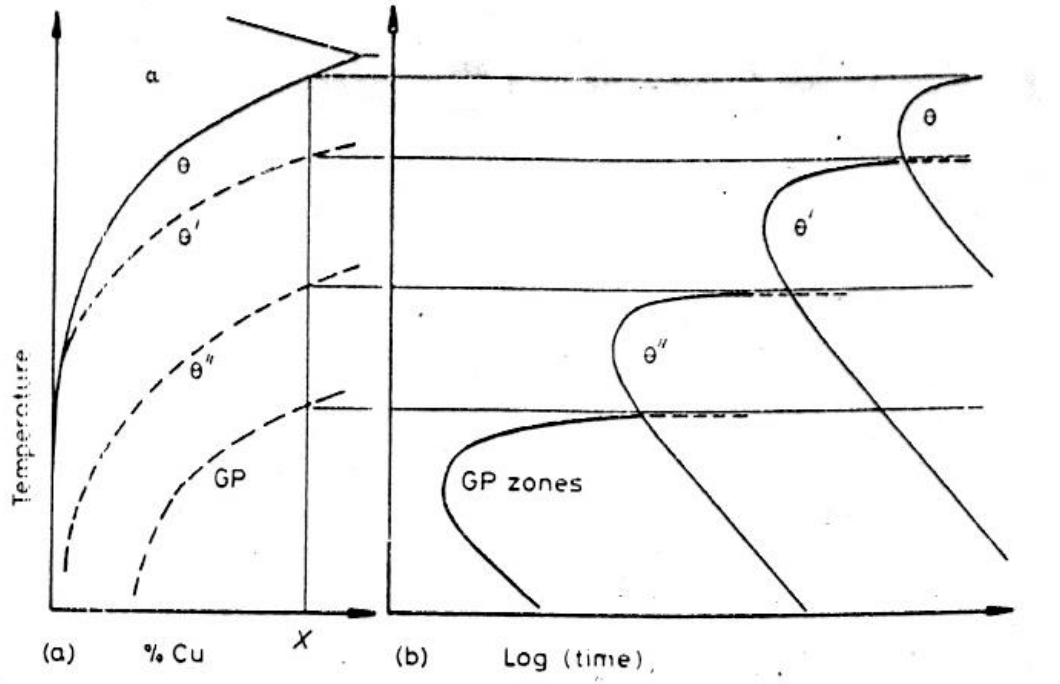

Fig. 5.32 (a) Metastable solvus lines in Al–Cu (schematic). (b) Time for start of precipitation at different temperatures for alloy X in (a).

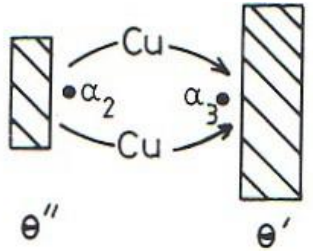

θ nucleates on gb’s and θ’- α interfaces.

Solvus lines and TTT curves can be drawn for all transition phases.

Age hardening Al-Cu alloys

Hardening curves depend on composition and annealing temperature (extent and type of transition phases). Hardening effects are

- solid solution hardening after quench,
- hardening by means of coherent zones
- effect of stress needed for dislocation to cut precipitate
- effect of pinning dislocation between precipitates (Orowan stress)

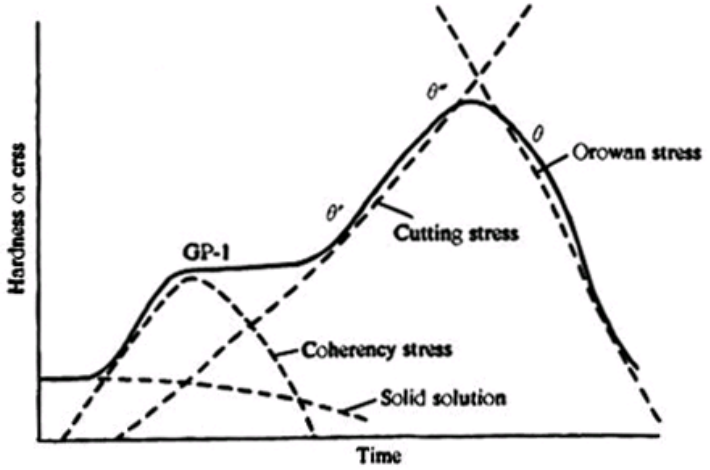

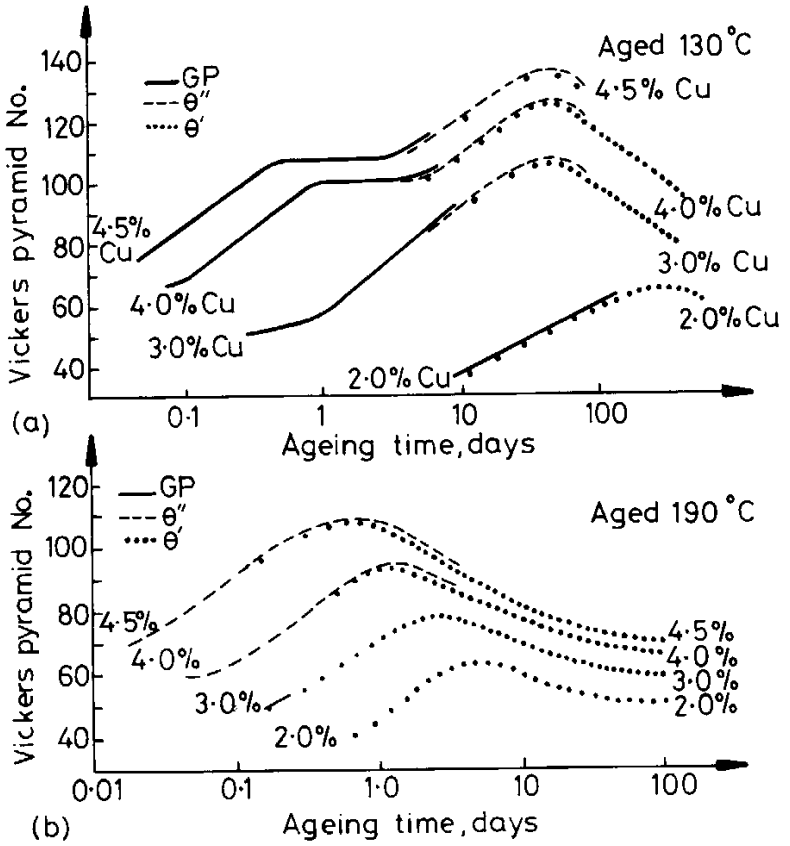

Annealing effects

Precipitation sequence is modified by ageing at temperatures between two solvuses.

Reversion: GP zones aged above their solvus dissolve.

Two stage annealings: nucleation at relatively low temperature (high frequency, low growth rate) + growth at higher temperature (short times).

Precipitate free zones (PFZ).

- preferential nucleation on gb's causing depletion of solute in neighbouring areas.

Fig. 5.36 PFZs around grain boundaries in a high-strength commercial Al–Zn–Mg–Cu alloy. Precipitates on grain boundaries have extracted solute from surrounding matrix. (×59 200)

Annealing effects

PFZ also caused by vacancy annihilation on gb's. Width depends on vacancy concentration profile: below critical concentration there is no nucleation of precipitates.

To reduce effect: increase solubilization temperature (induce higher vacancy content), faster quench (retain more supersaturated vacancies), age at lower temperature (increase nucleation frequency).

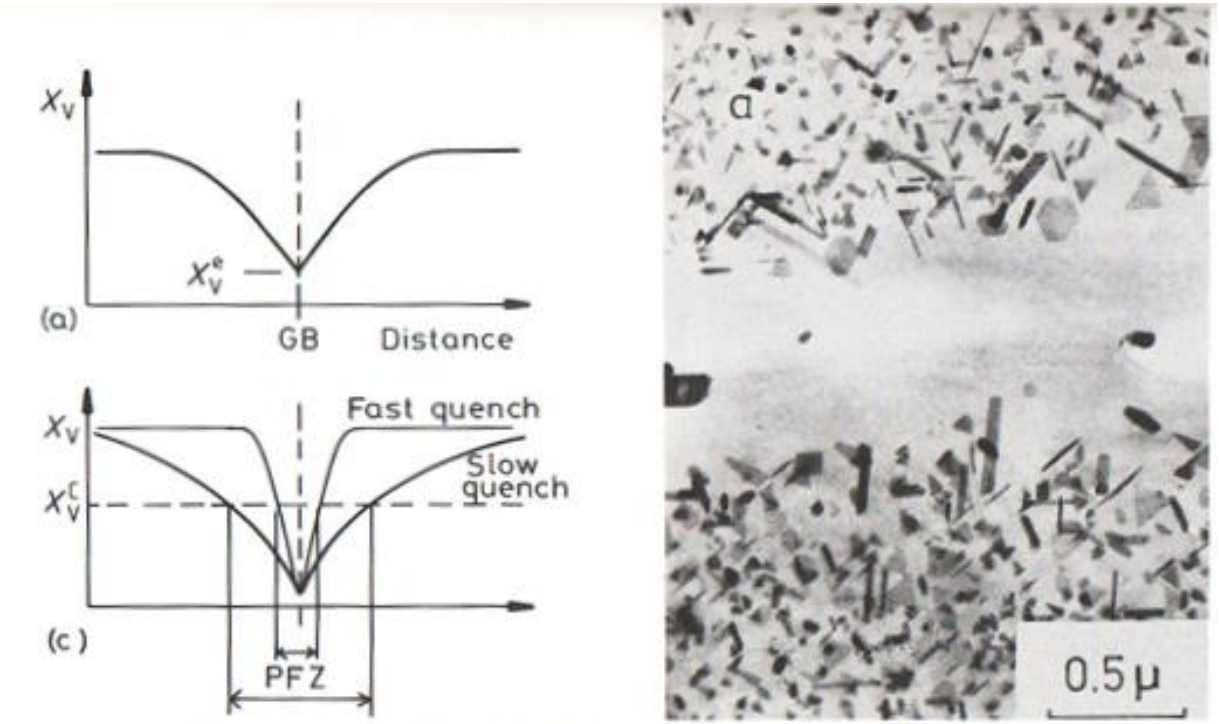

Fig. 5.35 A PFZ due to vacancy diffusion to a grain boundary during quenching. (a) Vacancy concentration profile. (b) A PFZ in an Al–Ge alloy (× 20 000). (c) Dependence of PFZ width on critical vacancy concentration X_V^c and rate of quenching.